JOURNAL OF APPLIED POLYMER SCIENCE VOL. 14, PP. 3049-3063 (1970)

A Micro-Macro Correlation of Ozone-Induced Fracture in Rubber

K. L. DeVRIES, E. R. SIMONSON, and M. L. WILLIAMS, *College of Engineering, University of Utah, Salt Lake City, Utah 84112*

Synopsis

Rate of molecular bond rupture is successfully correlated by a Griffith-type energy balance to the strain energy release rate during ozone cracking of rubber. Rate of bond rupture is determined from electron paramagnetic resonance (EPR) measurements. The rate of strain energy release is determined from stress–elongation measurements during stress relaxation, creep, and cyclic loading tests. To compare with macroscopic crack studies, it was assumed that each ruptured bond created a given amount of fracture surface. Numerical agreement could be obtained by assuming each broken bond results in the production of an area of approximately 10^{-13} cm^2. Using the surface energy density determined from stress relaxation tests in an energy balance gives surprisingly accurate predictions of expected behavior in creep and cyclic loading tests. There is a one-to-one correspondence between the rate of crack growth (bond rupture) and rate of energy release from strain and external work in all cases. It is proposed that such correlations give credence to a Griffith-type approach to environmental cracking which it did not have previously.

INTRODUCTION

Energy approaches to fracture have been extremely fruitful in their application to a variety of fracture phenomena including brittle-ductile fracture in metals,[1,2] fracture in elastic and viscoelastic polymers,[3,4] and environmental stress cracking of polymers.[5] The first successful attempt to use an energy approach to fracture was given by Griffith[6] in which he deduced that fracture (creation of new surface in a material) would occur when an infinitesimal increase of a crack would release more elastic strain energy than the energy Γ required to create new surfaces. The elastic solution for the stress field about a sharp V-notch crack becomes unbounded with an inverse square root strain singularity in the vicinity of the crack tip for even the smallest applied load.[7] It therefore appears that instantaneous fracture would occur and that the elastic stress analysis solution cannot be used to predict a critical bounded stress above which fracture is unavoidable. Griffith[6] considered the integrated strain energy, however, and neatly circumvented the difficulty by balancing, at fracture, the change of strain energy with incremental crack growth against the energy required to create new fracture surface. His well-known result predicted a finite applied tensile stress, σ_c, to initiate fracture

$$\sigma_c = \left(\frac{2E\gamma_c}{\pi a}\right)^{1/2} \tag{1}$$

where E is Young's modulus, γ_c is the energy required to create new cohesive fracture surface, and $2a$ is the finite length of the crack in a thin brittle sheet.

In a brittle material, all of the deformations are assumed to be elastic, and the input work to the material is converted to kinetic energy of crack propagation and the energy to create new surface. In other materials that exhibit plastic deformation or time-dependent viscous effects, one would expect to find additional energy sinks to absorb the plastic work and viscous dissipation. A number of investigators have successfully incorporated the viscous and ductile terms into the Griffith formulation by substituting for the fracture energy density γ a summation of the individual dissipative term,[4,8] i.e.,

$$\gamma = \gamma_b + \gamma_d + \gamma_v + \gamma_{KE} \tag{2}$$

where the subscripts b, d, v, and KE refer to brittle, ductile, viscous, and kinetic energy, respectively. The brittle term γ_b does not always dominate the series as it does for brittle fracture. Orowan,[1] for example, showed that in ductile metals and some polymers (PMMA), the plastic work term γ_d is usually much larger than the other terms, i.e., the majority of the work done by the propagating crack is dissipated as irrecoverable plastic flow near the tip of the crack.[1,2,9] It is conceivable that a reactive atmosphere might supply energy to a propagating crack in addition to the energy released by the strain field. In this way there might be an "effective" decrease in the total fracture work term γ, eq. (2). This phenomenon is commonly encountered in metals, glasses, and polymers when the material fractures under comparatively small stresses after being exposed to corrosive or chemically active environments.[10,11] As a specific case, unsaturated compounds (double carbon–carbon bonds) are readily attacked by ozone at the double bond site, usually resulting in complete scission.[12] Extreme surface degradation is observed in many unsaturated rubbers under small strain in an ozone environment. Very little elastic strain energy is required to create fracture surfaces from ozone cracking as compared to the strain energy required to tear the rubber in the absence of ozone. The fracture energy for ozone cracking is on the order of 100 ergs/cm^2,[5,13,14] while for tearing in the absence of ozone it is on the order of 10^6 to 10^7 ergs/cm^2.[15] It is, therefore, evident that the presence of ozone virtually reduces the fracture energy by four or five orders of magnitude. Because of the popularity of the Griffith approach to fracture, it is useful to examine the comparisons and correlations which can be obtained between electron paramagnetic resonance (EPR) studies and such an energy balance. EPR provides insights into atomic occurrences. We will attempt here to relate them to macroscopic failure through an approximate energy balance of the Griffith type.

OUTLINE OF EPR WORK

Electron paramagnetic resonance (EPR) has proved to be an extremely sensitive technique for studying ozone exposure cracking of rubber. EPR is basically a form of microwave absorption spectroscopy in which the presence of unpaired electrons (free radicals) can be detected if a sufficient number (threshold $\simeq 10^{12}$ free radicals/cm^3) are present. Experimentally such free radicals were found in ozone-degraded acrylonitrile–butadiene (Hycar 1043), *cis*-polybutadiene (CB 220), and natural rubber. The free radicals were readily formed in the stressed rubbers in sufficient number to be detected within 1 sec after exposure to an ozone concentration of 2.8 mg/l. Changes in the ozonated rubber EPR spectra at constant stress are shown in Figure 1. Furthermore, it was found experimentally that the total number of free radicals provided an indirect measure of the number of ruptured polymer chains.[16] In particular, the number of free radicals produced from ozone-degraded Hycar 1043 in an ozone concentration of 2.8 mg/l. was determined empirically to be linearly proportional to the stretch ratio λ, i.e.,

$$\begin{aligned} \frac{dN'}{dt} &= 0.292\ (3.32\lambda - 3.78)\times 10^{15}\ \text{spins/min} \quad \lambda \geq 1.13 \\ \frac{dN'}{dt} &\simeq 0 \qquad\qquad\qquad\qquad\qquad\quad \lambda < 1.13 \end{aligned} \tag{3}$$

where N' is the total number of free radicals produced within a volume $V_0 = 2.76\times 10^{-3}$ in.^{3} and λ is the stretch ratio (1 plus the strain). These data are consistent with observations on the macroscopic level, i.e., it is established that there is a threshold strain usually varying from 5 to 15% strain below which cracks do not propagate in a rubber.[17–20] Equation (3) exhibits the same effect in that below $\lambda = 1.13$ no free radicals are produced. Experimentally the absence of free-radical production was indicative of no ozone cracking.

In contrast to the studies briefly outlined above, a number of other investigators have studied ozone cracking on the macroscopic level by studying the characteristics of a single propagating crack,[5,18] while others have looked at the overall change in ozone cracks per unit area.[14,17,21] It was, therefore, thought that it might be interesting to relate atomic fracture (free-radical formation) to macroscopic fracture phenomena. Since ozone fracture is time dependent, it is believed to be more appropriate to use the reasonably general thermodynamic power equation for fracture[4]

$$\dot{I} = \dot{F} + 2D + \dot{K} + \dot{\Gamma} \tag{4}$$

which states that the rate of work input into a system, $\dot{I}$, must equal the rate of storing free energy, $\dot{F}$, plus the dissipation, $2D$ plus the rates of

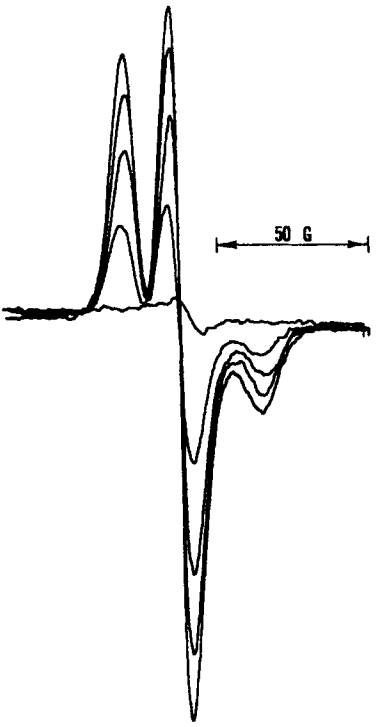

Fig. 1. Growth of EPR spectra of acrylonitrile–butadiene during ozone attack, with the lowermost curve being the residual signal. Each spectrum was drawn 5 min after preceding one.

converting kinetic energy, $\dot{K}$, and surface energy, $\dot{\Gamma}$. Specifically, using the notation of Sokolnikoff,[22]

$$\dot{I} = \int_A T_i \dot{u}_i dA \tag{5}$$

$$2D + \dot{F} = \frac{d}{dt}\int_V \int_0^t \sigma_i \dot{\epsilon}_i dt dV \tag{6}$$

$$\dot{K} = \frac{d}{dt}\int_V \int_0^t \rho \dot{u}_i \ddot{u}_i dt dV \tag{7}$$

$$\dot{\Gamma} = \frac{d}{dt}\int_A \gamma(t) dA \tag{8}$$

where A and V are the (time-dependent) areas and volumes, respectively. Even though the stress analysis is somewhat simplified in treating a uniaxial test with the cracks running perpendicular to the direction of elongation, the true stress distribution throughout the multicracked sample cannot be calculated analytically except in principle. To further complicate the problem, the region over which the integration of eqs. (6) and

(7) takes place continually changes with time owing to the multitude of cracks propagating through the body. We are, therefore, led to an ad hoc approximate formulation of the problem. As a first approximation, the dissipation (mechanical and thermal conversion into heat) and the kinetic energy changes are neglected. This is not to imply that there is no dissipation whatever, but we are assuming that the plastic and viscoelastic contributions are small. Experimentally, the stress was observed to relax less than 5% per hr in the absence of ozone. The hysteresis during loading was also of this order of magnitude. Equation (4) then becomes

$$\dot{I} = \dot{F} + \dot{\Gamma} \tag{9}$$

Superficially, this equation appears like purely elastic behavior. If such were the case, it would appear contradictory to consider time effects. The time dependence, however, results from the time-dependent ozone-induced cracking. The exact determination of $\dot{F}$ by integrating the strain energy density over the volume is intractable. As a first approximation, however, F will be replaced by the instantaneous area under the force–elongation curve, a form of Clapeyron's theorem.[22] This calculation can be made either by numerical integration or by integrating an appropriate analytical representation of the curve. Numerical integration was abandoned in favor of the second alternative, since the rubber samples used in these studies could be approximated quite well by the rubber elasticity equation of state for uniaxial loading[16,23]:

$$\sigma = nkT[\lambda - (1/\lambda^2)] \tag{10}$$

where σ is the engineering stress (load divided by the original cross-sectional area), n is the crosslink density (or perhaps more properly the number of elastically effective network chains per unit volume), k is Boltzmann's constant, T is the absolute temperature, and λ is the stretch ratio. This equation was also found to be a good approximation for the stress–strain curve for ozone-cracked rubber, provided nkT was replaced by an effective relaxation modulus, $n(t)kT$, with $n(0)$ being the modulus of the virgin sample. The effective crosslink density $n(t)$ is a decreasing function of time due to the increasing number of surface cracks. Incorporating this time dependence into eq. (10) yields

$$\sigma(t,\lambda) = n(t)kT[\lambda - (1/\lambda^2)] \tag{11}$$

It is appropriate at this time to discuss the surface energy term Γ in which $\gamma(t)$ is the energy to create a unit surface of newly fractured area and dA/dt is the rate of creation of the new area. The $\gamma(t)$ value is a property of the material and can be associated with the mechanism of energy dissipation in the body. Since fracture is the creation of new surface area from crack propagation and crack propagation results from bond rupture, the fracture work could as well be given in terms of energy per ruptured bond. Likewise, dA/dt could be given as dN/dt where N is the number of ruptured polymer chains. Converting from the one

relation to the other involves the amount of surface area generated when a polymer chain fractures. On the average, each chain that is ruptured creates a given amount of new surface area. This effective cross-sectional area for an amorphous polymer has been reported to be approximately 0.5×10^{-14} cm^2.[24] Thus, eq. 8 may be approximated as either

$$\frac{d\Gamma}{dt} = \gamma_n(t)\,\frac{dN}{dt} \tag{12}$$

or, in the alternate form of eq. (8),

$$\frac{d\Gamma}{dt} = \gamma(t)\,\frac{dA}{dt} \tag{13}$$

where dN/dt is given by eq. (3) and dA/dt is merely dN/dt divided by the number of polymer chains crossing through a unit cross section which, for the time being, is assumed to be 2×10^{14} chains/cm^2. Therefore,

$$\begin{aligned} \frac{dA}{dt} &= 0.452\ (3.32\lambda - 3.78)\ \text{in.}^2/\text{min} && \lambda \geq 1.3 \\ \frac{dA}{dt} &\simeq 0. && \lambda < 1.3 \end{aligned} \tag{14}$$

Equation (9) will now be applied to a constant elongation test in which a rubber sample, Hycar 1043, is exposed to an ozone environment (concentration 2.8 mg/l.). For clarity, consider the sketches of Figure 2 with the corresponding behavior shown on the stress–elongation curve. For the

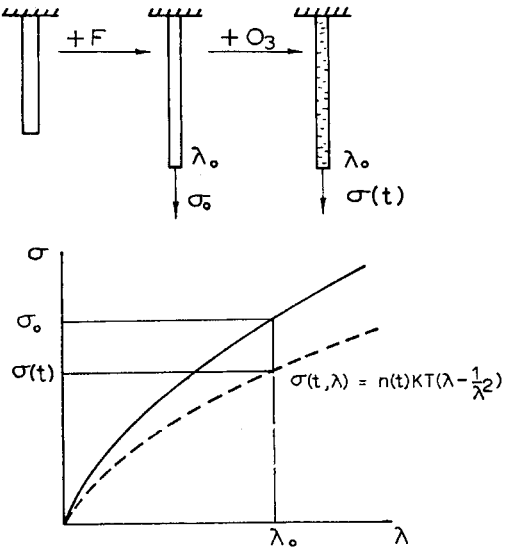

Fig. 2. Illustration showing the approximate stress–strain behavior for stress relaxation tests in an ozone environment.

above test after loading, no boundaries move; thus, no work is done, giving, from eq. (9),

$$\dot{F} = -\gamma(t)\frac{dA}{dt} \tag{15}$$

From the earlier assumption, $\dot{F}$ is approximated as

$$\dot{F} = V_0 \frac{d}{dt}\int_1^{\lambda_0} \sigma(t,\lambda)d\lambda \tag{16}$$

where V_0 is the volume of the sample which was assumed to be constant and equal to 2.76×10^{-3} in.^{3} Performing the indicated operations in eq. (16), one finds

$$\dot{F} = V_0\left(\frac{dn}{dt}\right)kT\left(\frac{\lambda^2{}_0}{2} + \frac{1}{\lambda_0} - \frac{3}{2}\right). \tag{17}$$

Combining eqs. (17) and (15),

$$\gamma(t) = \frac{V_0\left(\frac{dn}{dt}\right)kT\left(\frac{\lambda^2{}_0}{2} + \frac{1}{\lambda_0} - \frac{3}{2}\right)}{\frac{dA}{dt}}. \tag{18}$$

Multiplying by $\left(\lambda_0 - \frac{1}{\lambda_0{}^2}\right)$ gives $\gamma(t)$ as follows:

$$\gamma(t) = \frac{\frac{d\sigma}{dt}\left(\frac{\lambda^2{}_0}{2} + \frac{1}{\lambda_0} - \frac{3}{2}\right)V_0}{\frac{dA}{dt}\left(\lambda_0 - \frac{1}{\lambda^2{}_0}\right)}. \tag{19}$$

To this point, γ has been permitted to vary with time.* However, the measured stress relaxations $d\sigma/dt$ (see Figs. 3, 4, and 5) and the empirical equation dA/dt, eq. (14), are approximately independent of time in the range studied, which post facto is an indication of the elastic nature of the material. At a first glance, γ as given by eq. (19) appears to be a rather strong function of λ^0. However, empirically it was determined that the λ_0 dependence of dA/dt and $d\sigma/dt$ was such that the resulting γ was relatively constant. For example, substituting the experimental data for Hycar 1043 into eq. (19) yields $\gamma = 465 \pm 14\%$ ergs/cm^2. (This 14% does not represent the standard deviation but rather includes the complete experimental range and values of γ.) These γ values were for stretch

* In a known linearly viscoelastic material, the cohesive energy density actually is time (and temperature) dependent. For the butadiene–acrylonitrile–acrylic acid terpolymer crosslinked with an epoxy curing agent material, Bennett, Anderson, and Williams[28] found the dependence to follow the same time–temperature shift relation as did the relaxation modulus of the material.

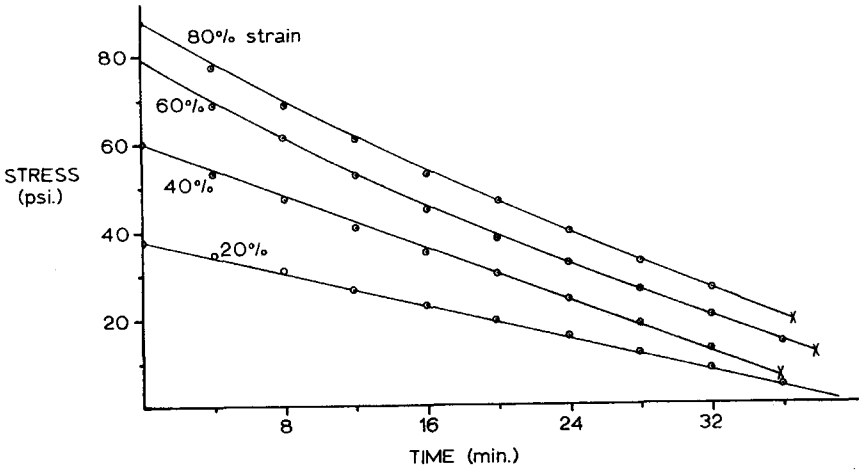

Fig. 3. Stress relaxation curves for acrylonitrile–butadiene (Hycar 1043). Ozone concentration 2.8 mg/l.; (X) catastrophic fracture point.

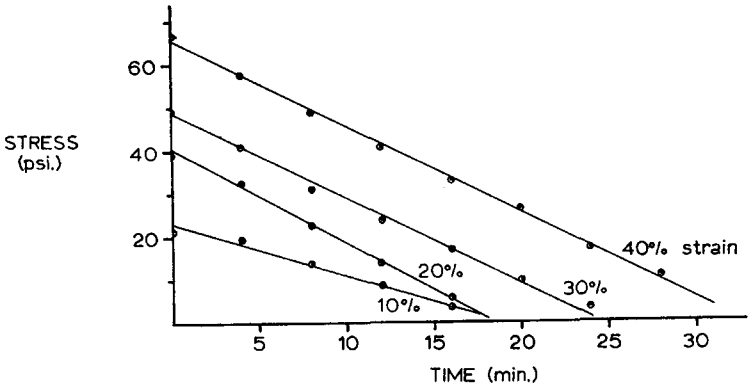

Fig. 4. Stress relaxation curves for *cis*-polybutadiene (CB 220). Ozone concentration 2.8 mg/l.

ratios between 1.2 and 1.8, with slight tendencies of larger γ values at lower stretch ratios. Considering the empirical nature of this result, it is felt that such a variation is within experimental error. Indeed, the variation is much less than that reported in the literature measured by other means.[5,19,25]

It should be noted that the value of γ determined here is somewhat higher than the values (50 to 120 ergs/cm^2) determined by observations of macroscopic cracks.[5,19,25] This difference could easily lie in the fact that the area created per ruptured bond differs from that assumed. If, for example, cracks were to selectively follow paths where fewer bonds are broken per area of fracture surface, then γ would be brought into better agreement. For the cases reported here, the cracks must choose a path

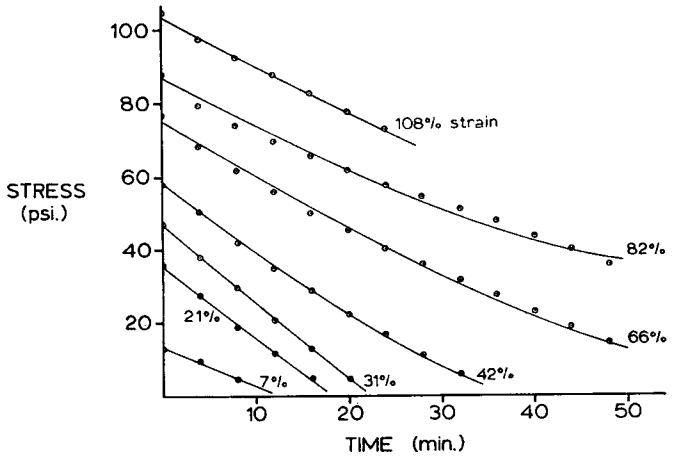

Fig. 5. Stress relaxation curves for natural rubber. Ozone concentration 2.8 mg/l.

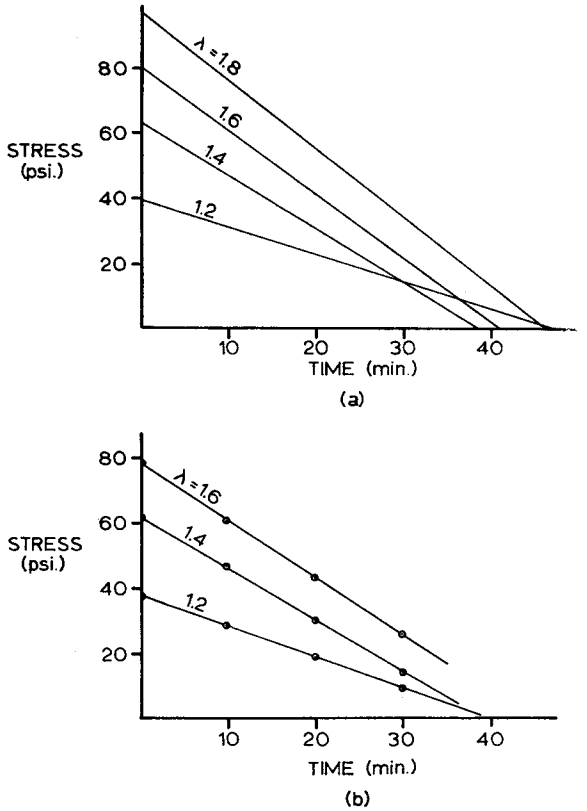

Fig. 6. Comparison of the theoretically calculated stress relaxation curves, eq. (20), with that measured experimentally on the acrylonitrile–butadiene gum rubber: (a) theoretical; (b) experimental; γ = 465 ergs/cm^2; ozone concentration 2.8 mg/l. Results are similar to those of Fig. 2 but are taken from a different "batch" of sample material.

fracturing roughly 25% as many broken bonds. There is strong evidence of a selective fracture path in semicrystalline polymers.[20,27] Therefore, it is reasonable to assume that the same might be true for an amorphous polymer.

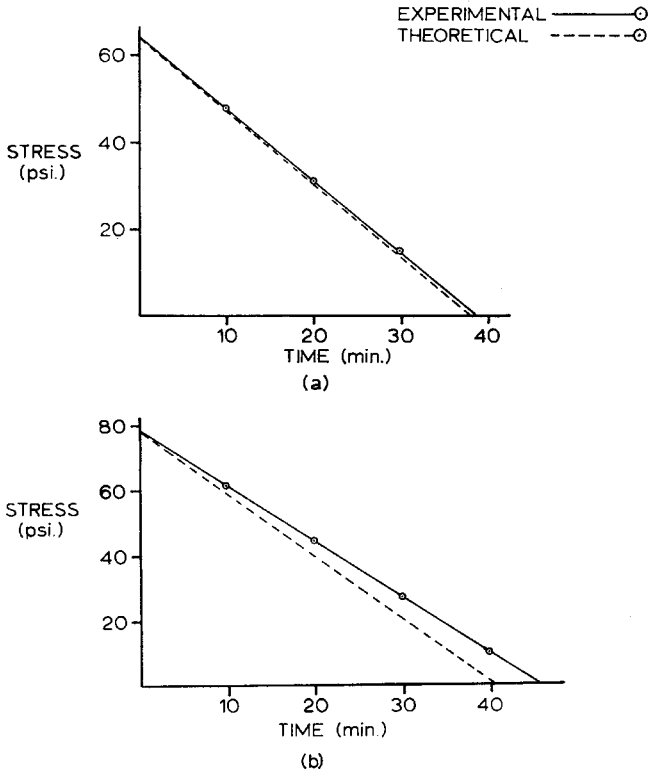

Fig. 7. Comparison showing the effect of varying the stretch ratio in eq. (20) with experimental relocation curves: (a) stretch ratio 1.4; (b) stretch ratio 1.6; γ = 465 ergs/cm^2 for theoretical curve.

Using γ = 465 ergs/cm^2 in eq. (19) gives the stress relaxation in a constant elongation test as follows:

$$\sigma(t,\lambda_0) = \sigma_0 - \frac{0.96\,[\lambda_0 - (1/\lambda^2{}_0)]A(t,\lambda)}{(\lambda^2{}_0/2) + (1/\lambda_0) - 1.5}\ \text{psi} \tag{20}$$

where σ_0, is n$(0,\lambda_0)$ and $A(t,\lambda_0)$ is the integral of eq. (14), i.e.,

$$A(t,\lambda_0) = \int_0^t 0.452(3.32\lambda_0 - 3.78)dt. \tag{21}$$

Equation (20) is plotted in Figure 6 along with the experimental data. Figure 7 shows the effect of varying γ in eq. (20).

APPLICATIONS TO OTHER LOADINGS

If the proposed model has a valid physical basis, then once γ has been determined from relaxation tests it should be possible to predict behavior under other loadings. Therefore, let us consider two other types of loading (creep and cyclic) and compare the theoretical predictions with experimental observations.

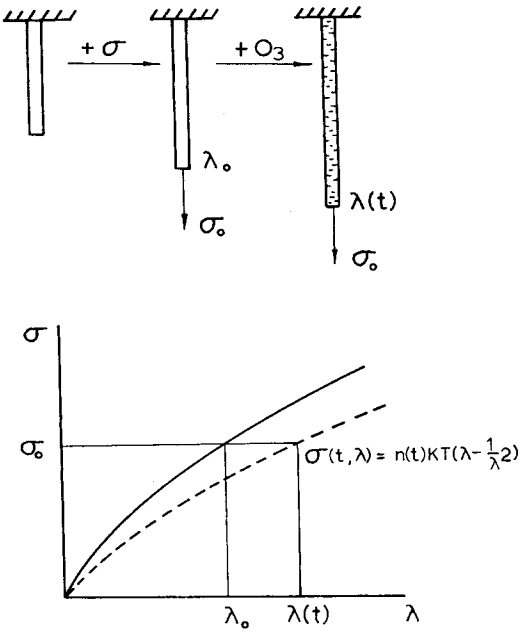

Fig. 8. Schematic representation of approximate stress–strain behavior for creep tests in an ozone environment.

Consider the schematic representation of a creep test as shown in Figure 8. For creep tests of this type, eq. (9) can be written as

$$\frac{d}{dt} V_0 \int_1^{\lambda} \sigma(t,\lambda) d\lambda + \gamma \frac{dA}{dt} = \frac{d}{dt} V_0 \int_{\lambda_0}^{\lambda(t)} \sigma_0 d\lambda. \tag{22}$$

Differentiating, one obtains

$$V_0 \left\{ \sigma[t,\lambda(t)] \frac{d\lambda}{dt} + \int_1^{\lambda(t)} \frac{\partial \sigma}{\partial t} d\lambda \right\} + \gamma \frac{dA}{dt} = V_0 \sigma_0 \frac{d\lambda}{dt}. \tag{23}$$

But for creep tests, $\sigma(t,\lambda(t)) \equiv \sigma_0$, so that

$$\int_1^{\lambda(t)} \frac{\partial \sigma}{\partial t} d\lambda = -\frac{\gamma}{V_0} \frac{dA}{dt}. \tag{24}$$

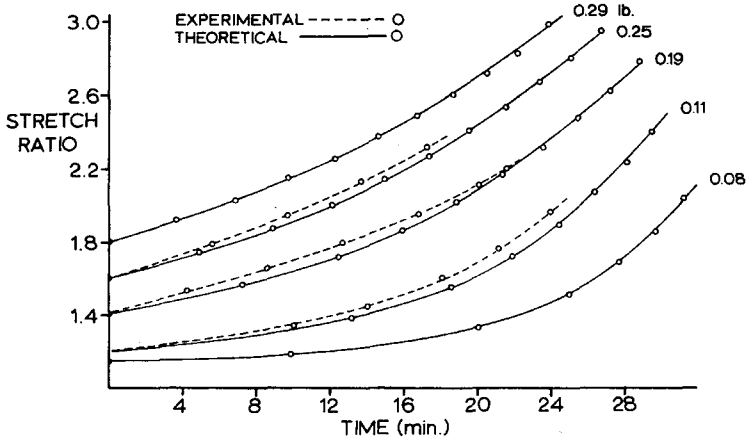

Fig. 9. Comparison of theoretically calculated creep curves, eq. (27), with those experimentally measured for acrylonitrile–butadiene (Hycar 1043) gum rubber: γ = 530 ergs/cm^2.

Integrating, we obtain

$$\frac{dn}{dt}(kT)\left(\frac{\lambda(t)^2}{2}+\frac{1}{\lambda(t)}-\frac{3}{2}\right)=-\frac{\gamma}{V_0}\frac{dA}{dt}. \tag{25}$$

The quantity $(dn/dt)(kT)$ can be calculated from eq. (11):

$$\frac{dn}{dt}(kT)=-\sigma_0\left(\frac{\lambda(t)^4+2\lambda(t)}{[\lambda(t)^3-1]^2}\right)\frac{d\lambda}{dt}. \tag{26}$$

Combining eqs. (25) and (26) results in the following equation relating $\lambda(t)$ to time:

$$\int_{\lambda_0}^{\lambda}\frac{(\lambda^3+2)(\lambda^3+2-3\lambda)}{(\lambda^6-2\lambda^3+1)(3.32\lambda-3.78)}d\lambda=\frac{0.994t}{\sigma_0} \tag{27}$$

where $\sigma_0=\sigma(0,\lambda_0)$. This equation was solved numerically and plotted with the experimental data shown in Figure 9. The results of the ad hoc energy formulation are encouraging in that the model using γ as determined in a stress relaxation test does appear to predict the correct behavior.

A similar energy balance can be applied to cyclic strains. Let us now investigate eq. (9) for solutions of cyclic strain test using γ = 465 ergs/cm^2. Consider the schematic shown in Figure 10.

Using $\lambda=\lambda_0+0.2\sin(6\pi t)$, eq. (9) becomes

$$\frac{d}{dt}\int_1^{\lambda_0+0.2\sin 6\pi t}\sigma(t,\lambda)d\lambda+\frac{\gamma}{V_0}\frac{dA}{dt}=\frac{d}{dt}\int_1^{\lambda_0+0.2\sin 6\pi t}\sigma(t),\sigma(t,\lambda)d\lambda. \tag{28}$$

Collecting terms and integrating, we obtain

$$\int_1^{\lambda_0}\sigma(t,\lambda)d\lambda=-\frac{\gamma}{V_0}A+C_1. \tag{29}$$

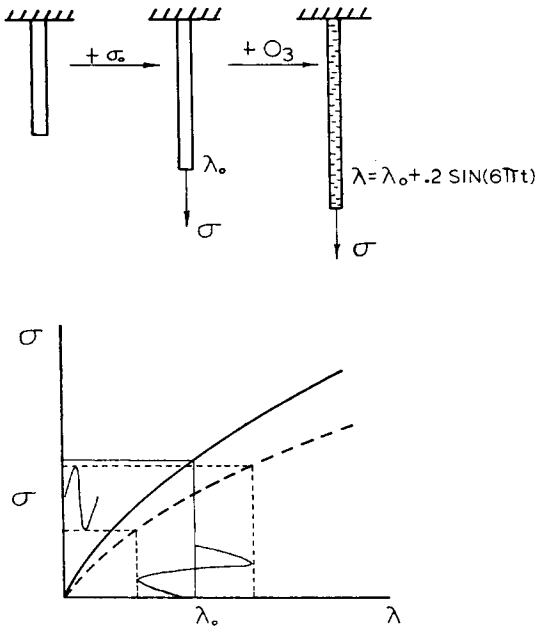

Fig. 10. Schematic representation of approximate stress–strain behavior for cyclic strain tests in an ozone environment.

Applying the initial conditions, $A = 0$ at $t = 0$, gives

$$C_1 = \int_1^{\lambda_0} \sigma(0,\lambda)d\lambda.$$

Substituting this value into eq. (29) and integrating results gives

$$[n(t)kT - n(0)kT]\left[\frac{\lambda_0^2}{2} + \frac{1}{\lambda_0} - \frac{3}{2}\right] = -\gamma A. \tag{30}$$

Multiplying both sides by $\lambda(t) - 1/[\lambda(t)]^2$ where $\lambda(t) = \lambda_0 + 0.2 \sin 6\pi t$, we obtain

$$\sigma[t,\lambda(t)] = \frac{\left[\lambda(t) + \frac{1}{\lambda(t)^2}\right]\left\{\left(\frac{\lambda_0^2}{2} + \frac{1}{\lambda_0} - 1.5\right)n(0)kT - \frac{\gamma}{V_0}A[t,\lambda(t)]\right\}}{\left[\frac{\lambda_0^2}{2} + \frac{1}{\lambda_0} - 1.5\right]} \tag{31}$$

where $\sigma[t,\lambda(t)]$ is the measured stress, A is given by eq. (21) with λ replaced by $\lambda = \lambda_0 + 0.2 \sin (6\pi t)$, and $n(0)kT$ is the initial value (66.9 psi) as determined from the stress–strain curve of the virgin rubber. Figure 11 shows eq. (31) with the experimental data. It may be further noted that changing the value of the fracture energy to only $\gamma = 400$ ergs/cm^2 in-

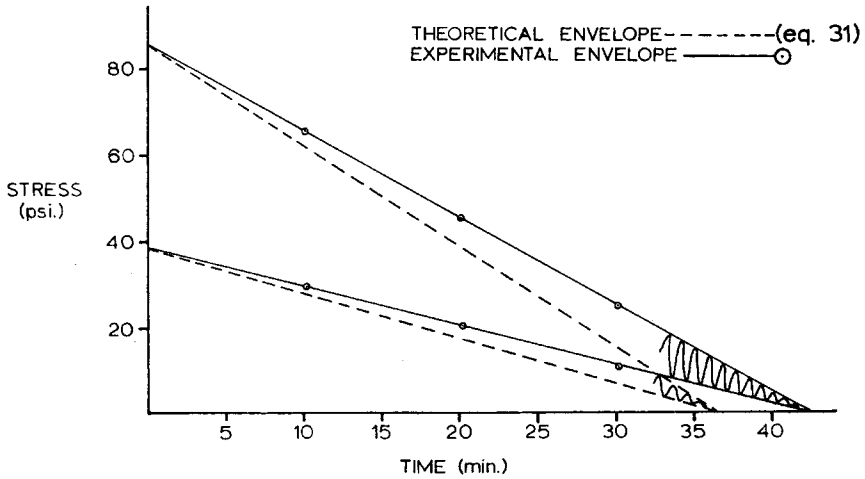

Fig. 11. Theoretical results as obtained from eq. (31) and experimental results for cyclic strain [$\lambda = 1.4 + 0.2 \sin(6\pi t)$] for the acrylonitrile–butadiene rubber: $\gamma = 465$ ergs/cm^2.

stead of 465 ergs/cm^2 (still within the 14% experimental variation in γ) resulted in a near perfect fit to the experimental data.

DISCUSSION

It appears that a good correlation between atomic phenomena and macroscopic fracture mechanics is possible. The results are internally very self-consistent. Cracks propagate (i.e., bonds rupture) only if and at rates dependent on the presence of sufficient strain energy. Numerical agreement between the value of critical energy obtained here and that obtained by others from macromeasurements can be achieved by assuming each ruptured bond on the average is equivalent to creating an area roughly three to five times the equivalent cross-sectional area of a polymer chain.

As noted previously, eq. (14), the rupture energy might equivalently be based on the number of broken bonds (ergs/bonds) rather than the amount of fracture area created (ergs/cm^2). If we assume that each ruptured bond results in one free radical detectable by EPR analysis, the apparent critical energy for bond rupture is approximately 5×10^{-12} ergs/bond in Hycar 1043. This compares very favorably with the bond energy of a covalent bond, i.e., 150 kcal/mole, or 10.8×10^{-12} ergs/bond. If one assumes that two free radicals are formed per chain scission (see ref. 16 for a discussion of this point), there is even better agreement. (It should perhaps be noted that some comparatively slow ozone attack does take place in unstressed rubbers. In an earlier paper[16] it was noted that this attack always rapidly decreased with time and was attributed to residually stressed bonds at the rubber surface.) We feel it too fortuitous for this numerical agreement and the other self-consistencies referred to

above all to be coincidental. Rather it appears that ozone causes rubber to fail in a brittle manner while supplying a small portion (50% or less) of the energy to rupture the bond. This agreement lends considerable credence to the Griffith-type approaches to ozone attack on rubbers. One might conjecture that the same type of approach should be applicable to other types of environmental stress cracking in elastomers. A critical test would be to investigate cracking under other types of loading such as torsion or biaxial stresses. Our equipment is presently being modified to conduct such experiments.

Portions of this work were sponsored by the National Aeronautics and Space Administration and the National Sciences Foundation.

References

1. E. Orowan, *Welding Res. Suppl.*, **20**, 57 (1955).
2. G. R. Irwin, *Fracturing of Metals*, Cleveland, American Society for Metals, 1948.
3. J. P. Berry, *J. Polym. Sci.*, **50**, 107 (1961).
4. M. L. Williams, *Int. J. Fract. Mech.*, **1**, 292 (1965).
5. M. Braden and A. N. Gent, *J. Appl. Polym. Sci.*, **3**, 100 (1960).
6. A. A. Griffith, *Phil. Trans. Roy. Soc., Ser. A*, **221**, 1963 (1921).
7. C. E. Inglis, *Trans. Inst. Nav. Architects*, **60**, 219 (1913).
8. W. Retting, *Rubber Chem. Technol.*, **40**, 1036 (1967).
9. L. J. Broutman and F. J. McGarry, *J. Appl. Polym. Sci.*, **9**, 589 (1965).
10. E. H. Andrews, *Fracture in Polymers*, New York, American Elsevier Publishing Company, 1968.
11. B. Rosen, *Fracture Processes in Polymeric Solids*, New York, Wiley, 1964.
12. P. S. Bailey, *Chem. Rev.*, **58**, 925 (1958).
13. G. J. Lake and P. B. Lindley, *J. Appl. Polym. Sci.*, **9**, 2031 (1965).
14. G. Salomon, and F. van Bloois, *J. Appl. Polym. Sci.*, **8**, 1991 (1964).
15. R. S. Rivlin and A. G. Thomas, *J. Polym. Sci.*, **10**, 291 (1953).
16. K. L. DeVries, E. R. Simonson, and M. L. Williams, *J. Macromol. Sci.*, in press.
17. R. Newton, *Trans. Inst. Rubber Ind.*, **21**, 113 (1945).
18. M. Braden, and A. N. Gent, *J. Appl. Polym. Sci.*, **3**, 90 (1960).
19. E. H. Andrews and M. Braden, *J. Polym. Sci.*, **55**, 787 (1961).
20. K. L. DeVries, E. R. Simonson, and M. L. Williams, Electron Paramagnetic Resonance Measurements of Strain-Induced Ozone Cracking in Rubber, Paper 69, MET-14, presented at meeting of American Society for Mechanical Engineers March 31 to April 2, 1969.
21. D. J. Buckley and S. B. Robinson, *J. Polym. Sci.*, **19**, 145 (1956).
22. I. S. Sokolnikoff, *Mathematical Theory of Elasticity*, New York, McGraw-Hill, 1956.
23. A. V. Tobolsky, *Properties and Structure of Polymers*, New York, Wiley, 1960.
24. A. Peterlin, *J. Polym. Sci.*, **7**, 1154 (1969).
25. E. H. Andrews, *J. Appl. Polym. Sci.*, **10**, 47 (1966).
26. D. K. Backman, An EPR Investigation of Polymer Fracture Surfaces, unpublished Ph.D. Dissertation, Department of Mechanical Engineering, University of Utah, June 1969.
27. A. Peterlin, *J. Polym. Sci.*, **7**, 1151 (1969).
28. S. J. Bennett, G. P. Anderson, and M. L. Williams, *J. Appl. Polym. Sci.*, **14**, 735 (1970).

Received January 20, 1970
Revised July 6, 1970